isolated ileal mucus samples from naïve mice (Fig. 2D), we did not detect *B. thetaiotaomicron* in our colony, suggesting that other commensals can induce epithelial fucosylation. To identify which indigenous bacteria are responsible for the induction of F-ECs, we analyzed mucus-associated bacterial populations residing in the mouse duodenum (part 1) and ileum (part 4). In contrast to the predominance of *Lactobacillus* in the duodenum, segmented filamentous bacteria (SFB) predominated in the ileum (Fig. 2D); this is consistent with previous studies (*23*, *24*). SFB are Gram-positive bacteria that preferentially colonize the epithelial surface of the terminal ileum, where they induce T helper 17 (T_H17) cells (*25*, *26*). Similar to their effect on T_H17 cell–inducing microbiota (*27*), vancomycin, ampicillin, and to some extent metronidazole—but not neomycin—extinguished epithelial fucosylation (fig. S1, B and C). Furthermore, consistent with the emergence of SFB, epithelial fucosylation is initiated after weaning (*6*, *28*). To investigate whether SFB have the potential to induce F-ECs, we examined mono-associated gnotobiotic mice and found that F-ECs were induced in SFB but not in *Lactobacillus murinus* mono-associated mice (Fig. 2E). Together, these results suggest that epithelial fucosylation in the terminal ileum is induced by commensal bacteria, including SFB, under physiological conditions.

ILC3 are required for epithelial fucosylation

We next investigated the cellular and molecular mechanisms of F-EC induction. Commensal bacteria, including SFB, induce the proliferation of intraepithelial lymphocytes and immunoglobulin A (IgA)–producing cells and the development of T_H17 cells; they also modulate the function of ILCs (*3*, *4*, *25*–*27*, *29*). To assess whether epithelial fucosylation is induced directly by commensal bacteria or is mediated by mucosal immune cells, we first analyzed the epithelial fucose status of T cell–, B cell–, and Rag-deficient mice. The number of F-ECs was not decreased in T cell– or B cell–deficient mice (fig. S2), indicating that T cells and B cells are dispensable for the induction of epithelial fucosylation. Although SFB induce T_H17 cells (*25*, *26*), T_H17 cells are not required for epithelial fucosylation because IL-6, a critical cytokine for T_H17 cell differentiation in the intestine (*30*), was also not necessary for the induction of F-ECs (fig. S3, A to C). We next analyzed RAR-related orphan receptor–γt (RORγt)–deficient mice, which lack the ILC3 subset, in addition to T_H17 cells (*30*, *31*). RORγt-deficient mice exhibited a marked decrease in the number of F-ECs, accompanied by a decrease in *Fut2* expression in ileal ECs (Fig. 3, A to D). These findings suggest that ILC3 are critical inducers of F-ECs. This was further supported by our observation of few F-ECs in the ileum of Id2-deficient mice, which do not develop any of the ILC subsets (Fig. 3, E to G) (*31*, *32*). Although both RORγt- and Id2-deficient mice lack PPs (*33*, *34*), PPs are not necessary for epithelial fucosylation because PP-null mice, generated by treatment with monoclonal antibody (mAb) to IL-7R during fetal growth, had normal levels of F-ECs (fig. S4). ILC3 in the small intestine are aberrantly expanded in Rag-deficient mice (*35*), and elevated numbers of F-ECs were observed in these mice (Fig. 3, H and I), supporting the notion that F-ECs are induced by ILC3. Because ILC3 express higher levels of CD90, they

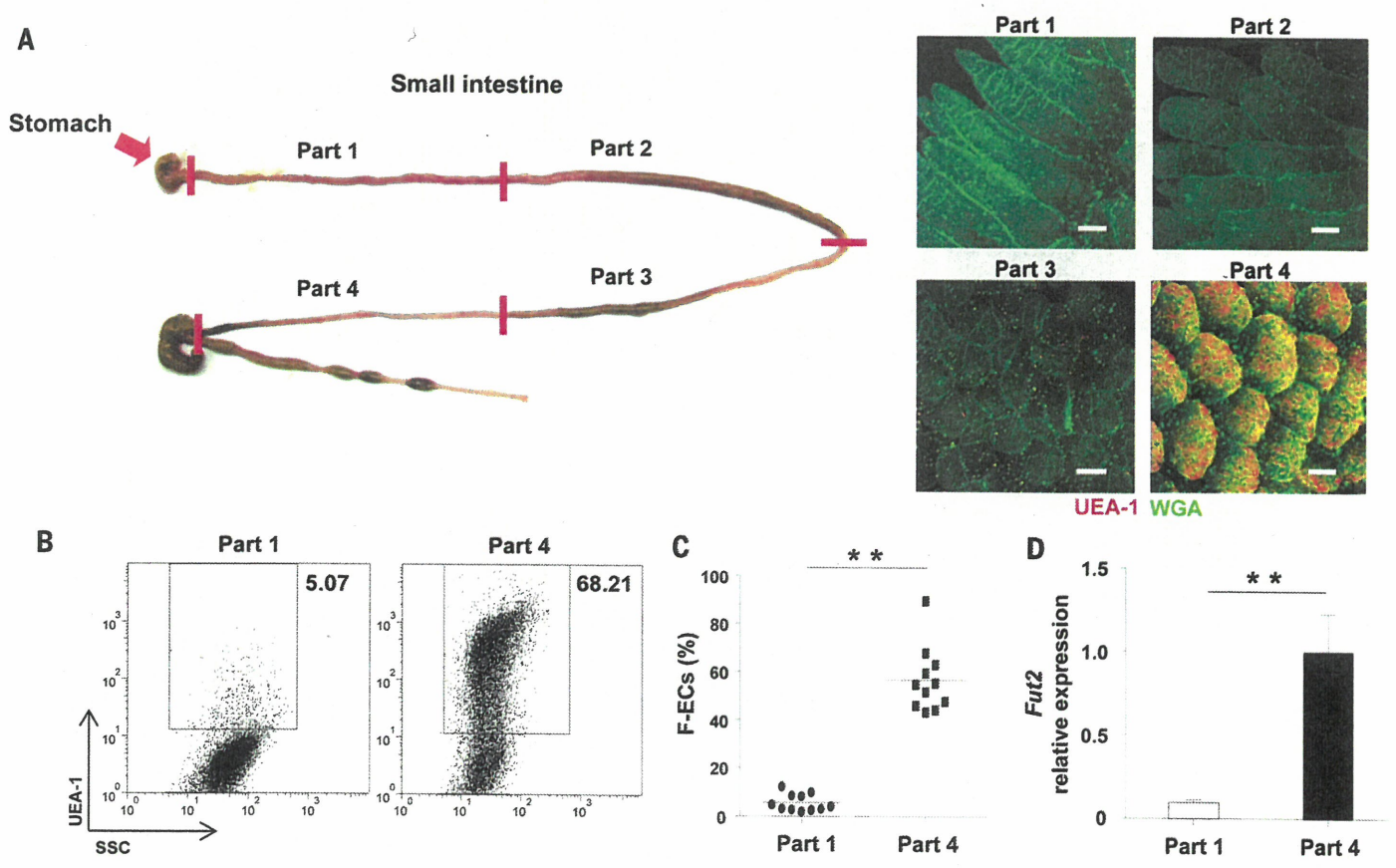

Fig. 1. F-ECs are dominant in the ileum. (**A**) Mouse small intestines were divided equally into 4 parts (parts 1, 2, 3, and 4), from the proximal (duodenum) to the distal (ileum) ends (left), and whole-mount tissues were stained with UEA-1 (red) and WGA (green) to detect F-ECs (UEA-1$^+$ WGA$^+$ cells) (right). Scale bars, 100 μm. Data are representative of three independent experiments. (**B** and **C**) Flow cytometric analysis of intestinal ECs isolated from part 1 and part 4 of the small intestines of C57BL/6 (B6) mice. Representative dot-plots are shown in (B). Percentages and mean numbers (horizontal bars) of fucosylated epithelial cells (n = 11 mice per group) are shown (C). SSC, side scatter. Data of two independent experiments are combined. (**D**) Expression of *Fut2* in ECs isolated from part 1 and part 4 of the small intestine isolated from five to six mice per group. Error bars indicate SD. $^{**}P < 0.01$ by using Student's t test. Data are representative of two independent experiments.

can be depleted with a mAb to CD90 (*36*, *37*). To identify whether ILC3 induce F-ECs, we treated wild-type and Rag-deficient mice with a mAb to CD90. *Fut2* expression and the number of F-ECs were markedly decreased after depletion of ILCs in both wild-type and Rag-deficient mice (Fig. 3, J to M, and fig. S5, A and B). Substantial numbers of SFB were still observed in RORγt-, Id2-, and CD90$^+$ ILC–depleted mice (fig. S6, A and B). Therefore, the defective epithelial fucosylation in these models was not attributable to the absence of F-EC–inducing commensals. Collectively, these results indicate that CD90$^+$ ILC3 are required for the induction and maintenance of F-ECs.

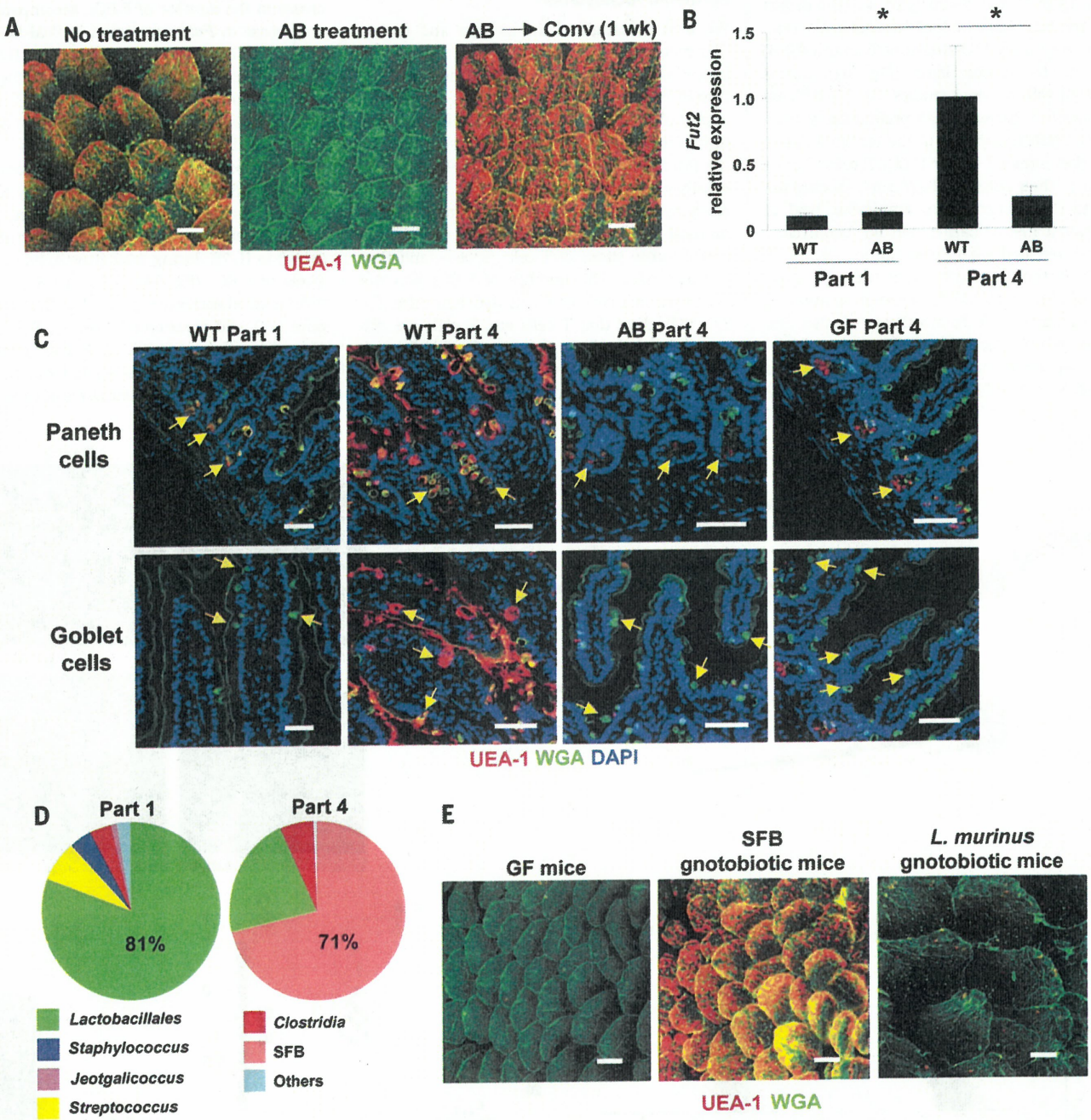

Fig. 2. Commensal bacteria induce epithelial fucosylation under homeostatic conditions. (**A**) Whole-mount ileal tissues of AB-treated mice and conventionalized AB-treated mice were stained with UEA-1 (red) and WGA (green) (n = 3 mice per group). Scale bars, 100 μm. Data are representative of two independent experiments. (**B**) *Fut2* expression in ECs isolated from part 1 (duodenum) and part 4 (ileum) of the small intestines of wild-type (WT) and AB-treated mice (n = 3 mice per group). Error bars indicate SD. *P < 0.05 by using Student's t test. Data are representative of two independent experiments. (**C**) Tissues from part 1 and part 4 of the small intestines of WT, AB-treated, and GF mice were stained with UEA-1 (red), WGA (green), and 4′,6-diamidino-2-phenylindole (DAPI) (blue). Arrows show Paneth cells (top) and goblet cells (bottom). Scale bars, 50 μm. Data are representative of two independent experiments. (**D**) Bacterial populations isolated from the mucus fraction of part 1 and part 4 of mouse small intestine were analyzed by means of 16S rRNA gene clone library. Representative graphs were constructed from samples (part 1, n = 480 clones; Part 4, n = 477 clones) isolated from five different mice (95 or 96 samples were obtained from each mouse). (**E**) Ileal tissues of GF, SFB, or *L. murinus* mono-associated mice (n = 3 mice per group) were stained with UEA-1 (red) and WGA (green). Scale bars, 100 μm. Data are representative of two independent experiments.

IL-22 produced by ILC3 mediates epithelial fucosylation

We next investigated how ILC3 induce epithelial fucosylation. ILC3 cells secrete IL-22, which stimulates the antimicrobial function and maintenance of intestinal ECs (*3*, *4*, *36*, *38*). Indeed, the expression of *Il22* gene was much higher in ILC3 than in any other intestinal immune cell subset (fig. S7A). We therefore assessed whether commensal bacteria regulate ILC3 differentiation and cytokine expression. Although AB-treated or wild-type mice had similar numbers of CD3$^-$ RORγt$^+$

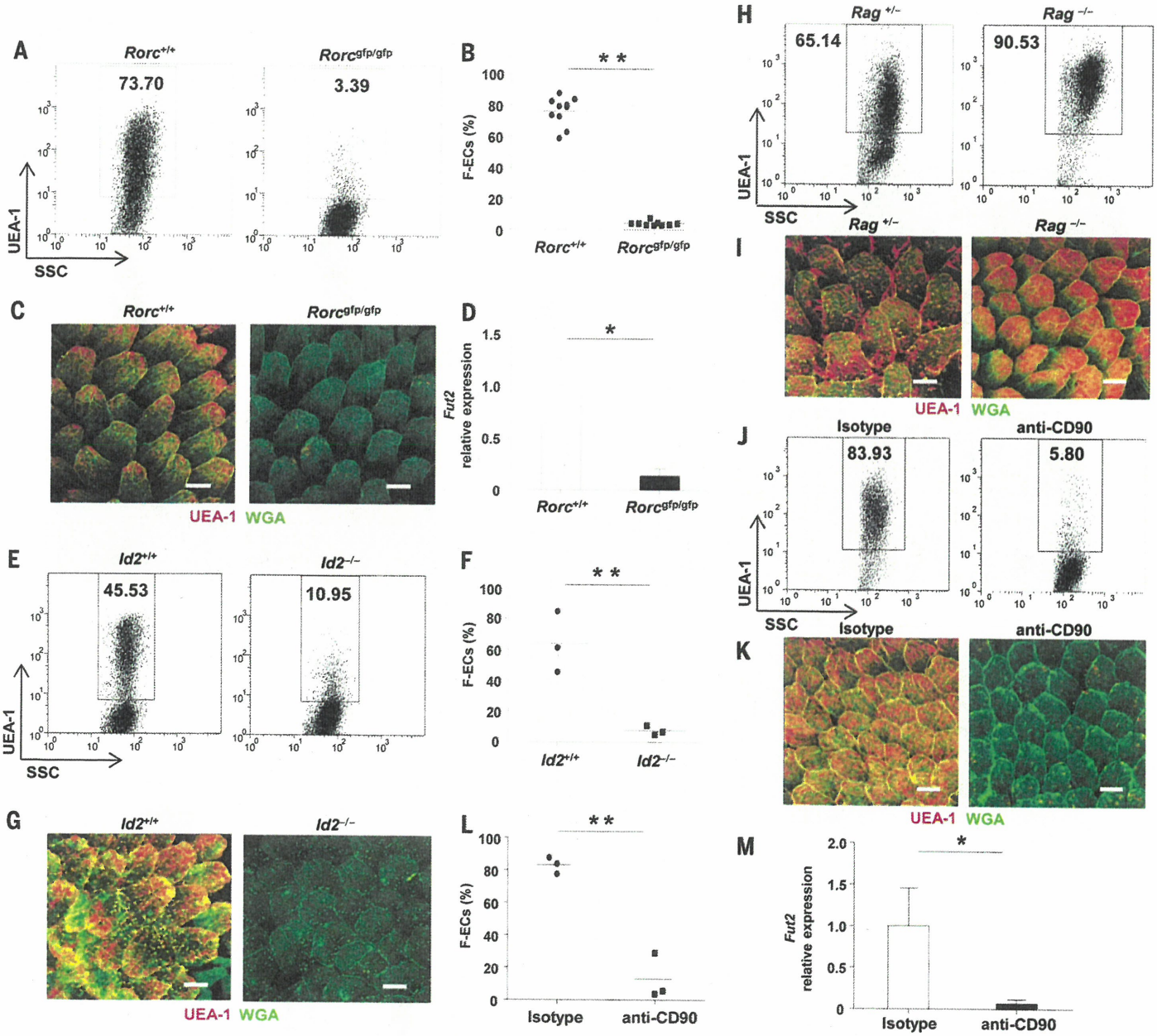

Fig. 3. CD90$^+$ RORγt$^+$ ILC3 induce F-ECs. (**A** and **B**) Representative dot-plots (A) and percentages and means (B) (horizontal bars) of ileal F-ECs isolated from *Rorc*$^{+/+}$ and *Rorc*$^{gfp/gfp}$ mice (n = 10 mice per group). SSC, side scatter. $^{**}P < 0.01$ by using Student's t test. Data of two independent experiments are combined. (**C**) Whole-mount ileal tissues from *Rorc*$^{+/+}$ and *Rorc*$^{gfp/gfp}$ mice were stained with UEA-1 (red) and WGA (green) (n = 10 mice per group). Scale bars, 100 μm. Data are representative of two independent experiments. (**D**) Expression of *Fut2* in ileal ECs isolated from *Rorc*$^{+/+}$ and *Rorc*$^{gfp/gfp}$ mice (n = 5 mice per group). Data are representative of two independent experiments. Error bars indicate SD. $^{*}P < 0.05$. (**E** and **F**) Representative dot-plots (E) and percentages and means (F) (horizontal bars) of ileal ECs isolated from *Id2*$^{+/+}$ and *Id2*$^{-/-}$ mice (n = 3 mice per group). Data of three independent experiments are combined. (**G**) Whole-mount staining of ileal villi isolated from *Id2*$^{+/+}$ and *Id2*$^{-/-}$ mice. Scale bars, 100 μm. Data are representative of three independent experiments. (**H** and **J**) Representative dot-plots of ileal ECs isolated from *Rag*$^{+/-}$ and *Rag*$^{-/-}$ mice (H) and *Rag*$^{-/-}$ mice treated with mAb to CD90 (anti-CD90 mAb) or isotype control Ab to CD90 (J) (n = 3 mice per group). (**I** and **K**) Whole-mount staining of ileal villi isolated from *Rag*$^{+/-}$ or *Rag*$^{-/-}$ mice (I) and anti-CD90 mAb– or anti-CD90 isotype control Ab–treated *Rag*$^{-/-}$ mice (K) (n = 3 mice per group). Scale bars, 100 μm. Data are representative of two independent experiments. (**L** and **M**) Percentages and means (horizontal bars) of ileal F-ECs (L) and *Fut2* expression (M) isolated from anti-CD90 mAb– or isotype control Ab–treated *Rag*$^{-/-}$ mice (n = 3 mice per group). Data are representative of two independent experiments. Error bars indicate SD. $^{*}P < 0.05$, $^{**}P < 0.01$ by using Student's t test.

ILC3 (fig. S7, B and C), expression of IL-22 was significantly reduced in AB-treated mice but was restored after cessation of AB treatment (fig. S7D). To identify whether IL-22 is involved in the induction of F-ECs, we analyzed mice lacking IL-22 and found that they had reduced numbers of F-ECs; this was correlated with a decrease in epithelial *Fut2* expression (Fig. 4, A and B). We next examined whether IL-22 alone induced epithelial fucosylation. We used hydrodynamic delivery of an *Il22*-encoding plasmid vector so as to ectopically overexpress IL-22 in AB-treated mice (fig. S8, A and B). In both AB-treated wild-type and $Rorc^{gfp/gfp}$ mice, F-ECs were induced in both the duodenum (part 1) and the ileum (part 4) in mice ectopically producing IL-22 but not in mice receiving control vector (Fig. 4, C and D, and fig. S8, C and D). This suggests that IL-22 is sufficient for epithelial fucosylation. Expression of *Fut2* was correlated with the presence of IL-22–induced F-ECs (Fig. 4E). To confirm whether IL-22 produced by ILC3 is necessary for epithelial fucosylation, Rag-deficient mice were treated with an antibody in order to neutralize IL-22. Epithelial *Fut2* expression and fucosylation were interrupted by the neutralization of IL-22 (Fig. 4, F to H). Microbial analyses of IL-22–deficient and

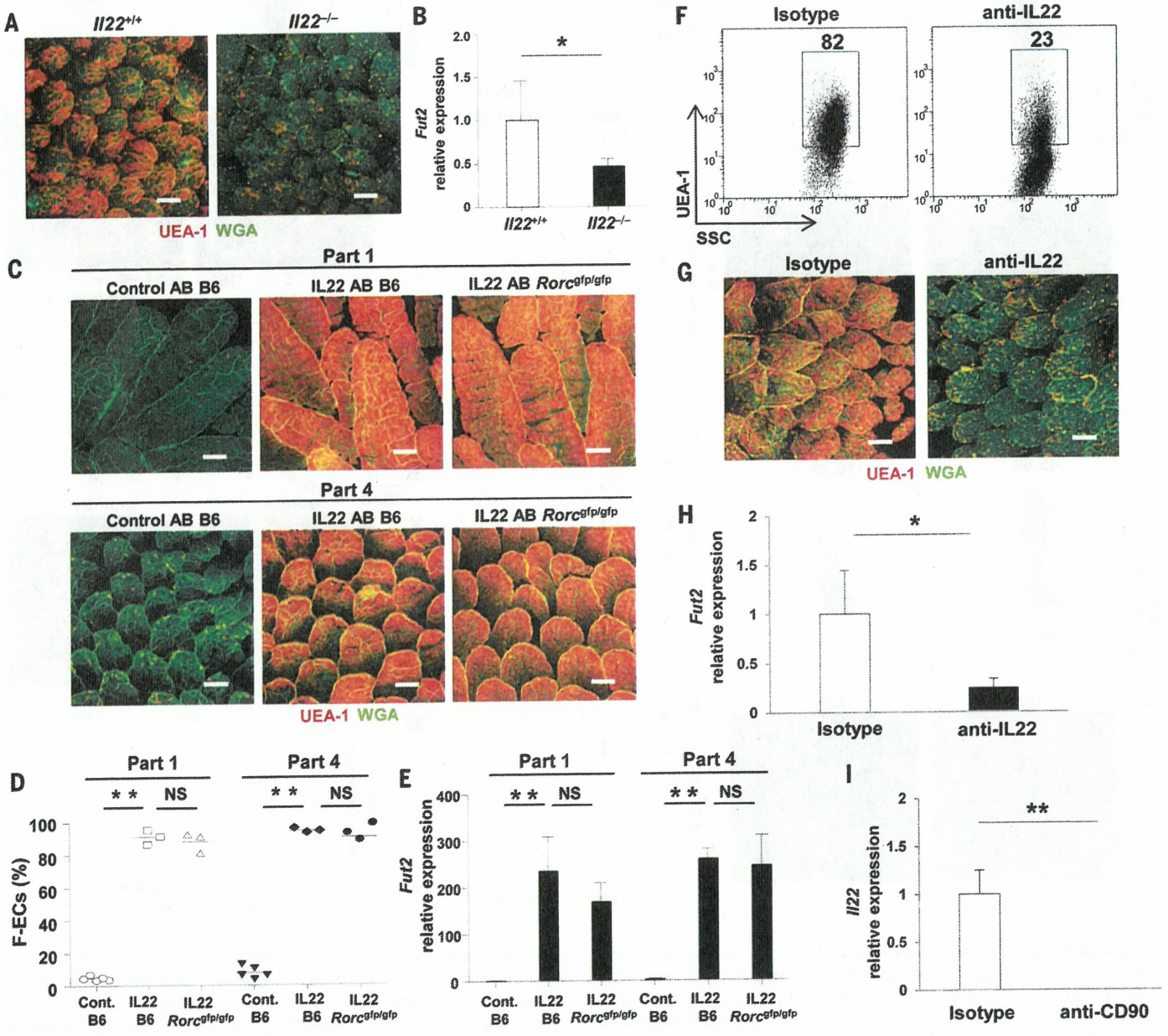

Fig. 4. IL-22 produced by ILCs is involved in the induction of F-ECs. (**A** and **B**) Whole-mount tissues stained with UEA-1 (red) and WGA (green) (A) and gene expression of *Fut2* (B) in ileal villi isolated from $Il22^{+/+}$ or $Il22^{-/-}$ mice (n = 6 mice per group). Error bars indicate SD. *P < 0.05 by using Student's t test. Scale bars, 100 μm. Data are representative of two independent experiments. (**C** to **E**) AB-treated C57BL/6 (B6) or $Rorc^{gfp/gfp}$ mice were intravenously injected with IL-22–encoding plasmid or control vector. Whole-mount staining (C), frequency of F-ECs (D) (mean, horizontal bars), and Fut2 mRNA expression was analyzed by means of rRT-PCR ($n \geq 3$ mice per group) (E). Scale bars, 100 μm. Error bars indicate SD. **P < 0.01 by using Student's t test. NS, not significant. Data are representative of two independent experiments. (**F** to **H**) Representative dot-plots (F), whole-mount histological images (G), and expression of *Fut2* (H) of ileal ECs isolated from $Rag^{-/-}$ mice treated with antibody to IL-22 or control Ab. Scale bars, 100 μm. Error bars indicate SD. *P < 0.05 by using Student's t test. (**I**) Expression of *Il22* in ileal LP cells from $Rag^{-/-}$ mice treated with antibody to CD90 or control Ab. Error bar inidicate SD. **P < 0.01 by using Student's t test. Data are representative of two independent experiments.

antibody-to-IL-22–treated Rag-deficient mice revealed the presence of SFB (fig. S6, A and B). These findings demonstrate that ILC3-derived IL-22 induced by commensal bacteria mediates epithelial fucosylation. Furthermore, depletion of ILC3 by injecting antibody to CD90 into Rag-deficient mice resulted in marked reduction of IL-22 expression (Fig. 4I), supporting the notion that IL-22–mediated signals produced by ILC3 are a key part of the EC fucosylation cascade. IL-22R is composed of two subunits, IL-22R1 and IL-10Rβ (*39*). Whereas IL-10Rβ was ubiquitously expressed, expression of IL-22R1 was specifically detected in intestinal ECs and was not reduced, even after the depletion of commensal bacteria (fig. S9, A and B). Taken together, our findings indicate that commensal bacteria provide signals that prompt ILC3 to produce IL-22, which leads to the induction of Fut2 by IL-22R–positive intestinal ECs.

LTα expressed by ILC3 induces epithelial fucosylation

ILC3 support the development and maintenance of secondary lymphoid tissues through the expression of lymphotoxins (LTs)—especially LTα1β2 (*40*). The expression of *Lta* and *Ltb* genes was higher in ILC3 than in any other intestinal immune cell subset (fig. S10A). In contrast to IL-22, which was induced by commensal bacteria, *Lta* and *Ltb* gene expression in ILC3 was not affected by commensal flora because the AB treatment did not alter the gene expression (fig. S10B). However, intestinal epithelial fucosylation and *Fut2* expression were severely impaired in $Lta^{-/-}$ mice (Fig. 5, A to C). $Lta^{-/-}$ mice possess congenital defects in secondary lymphoid organs (*41*). To elucidate the contribution of LTα to epithelial fucosylation in adult mice that have established secondary lymphoid organs, wild-type mice were treated with LTβR-Ig, which blocks LTα1β2 signaling. Epithelial fucosylation was attenuated by treatment with LTβR-Ig (Fig. 5, D to E), implying that a continuous LT signal is required for epithelial fucosylation. To investigate whether LTα in ILC3 is crucial for the induction of F-ECs, we constructed mixed bone marrow (BM) chimeric mice by transferring BM cells taken from

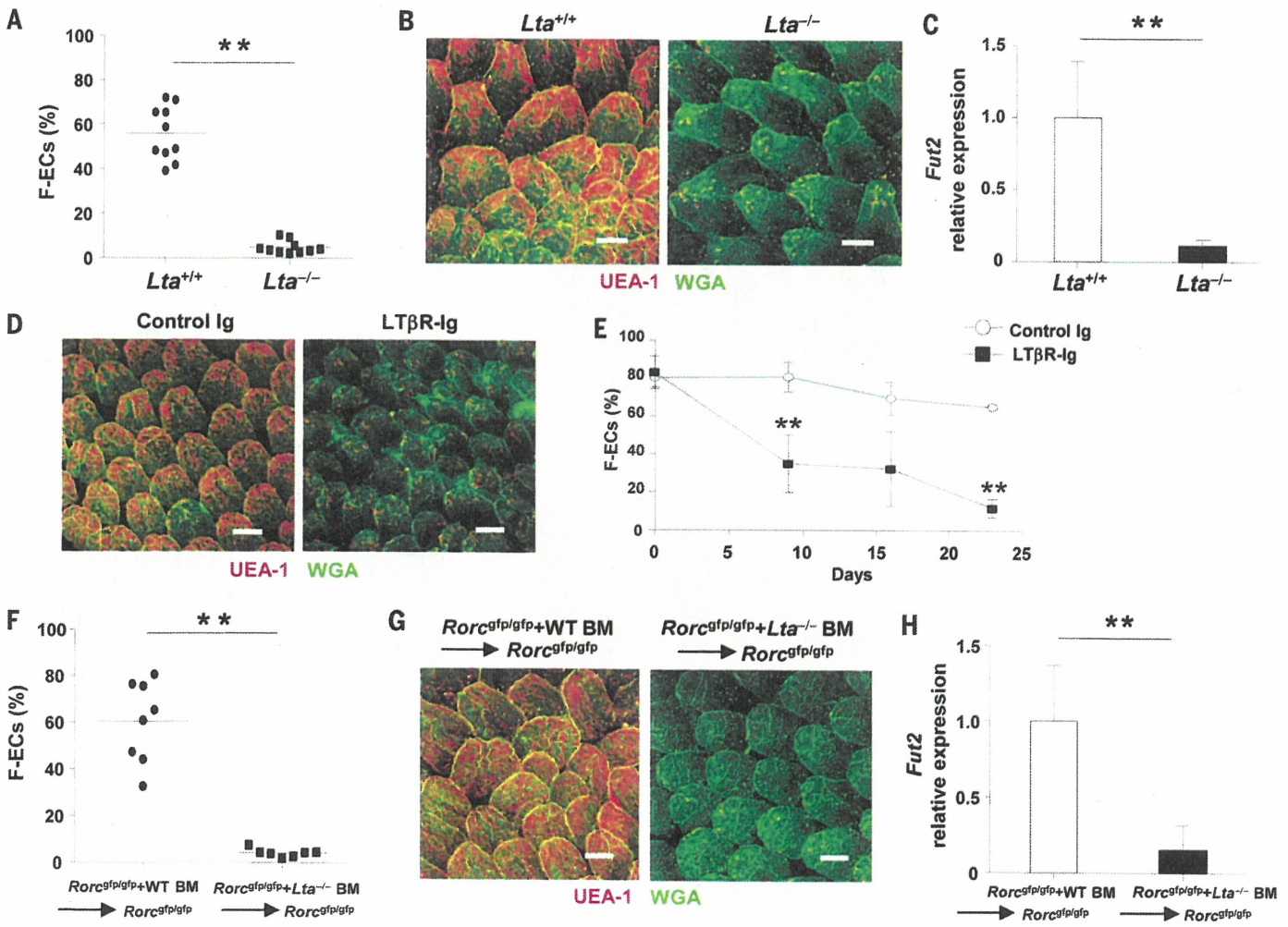

Fig. 5. LTs in innate lymphoid cells induce F-ECs. (**A**) Representative values and means (horizontal bars) of frequency of ileal F-ECs isolated from $Lta^{+/+}$ or $Lta^{-/-}$ mice (n = 10 mice per group). Data of two independent experiments are combined. $^{**}P < 0.01$ by using Student's t test. (**B**) Representative whole-mount staining of ileal villi isolated from $Lta^{+/+}$ or $Lta^{-/-}$ mice (n = 10 mice per group). Scale bars, 100 μm. (**C**) Expression of *Fut2* in ileal ECs isolated from $Lta^{+/+}$ or $Lta^{-/-}$ mice (n = 5 mice per group). Error bars inidicate SD. $^{**}P < 0.01$ by using Student's t test. Data are representative of two independent experiments. (**D**) Representative whole-mount staining of ileal villi from C57BL/6 mice injected with control IgG or LTβR-Ig. Tissues were stained with UEA-1 (red) and WGA (green). (n = 3 mice per group) (**E**) Frequencies of F-ECs in the ileum of C57BL/6 mice injected with control IgG (control Ab) or LTβR-Ig twice (day 9), 3 times (day 16), or 4 times (day 23) (n = 3 mice per group). Error bars indicate SD. $^{**}P < 0.01$ by using Student's t test. (**F** to **H**) Values and means (F), representative whole-mount staining (G), and expression of *Fut2* (H) in ileal ECs isolated from $Rorc^{gfp/gfp}$ mice injected with a mixture of BM cells from $Rorc^{gfp/gfp}$ and WT mice or $Rorc^{gfp/gfp}$ and $Lta^{-/-}$ mice (n = 7 to 8 mice per group). Data of two independent experiments are combined. Error bars indicate SD. $^{**}P < 0.01$ by using Student's t test. Scale bars, 100 μm.